ISTITUTO NAZIONALE FISICA NUCLEARE

INFN/AE - 82/13
6 Dicembre 1982

C. Cernigoi, R. Cherubini, D. Gill, N. Grion, G. Pauli and R. Rui:

SINGLE NEUTRON EMISSION FOLLOWING THE π^- ABSORPTION AT REST IN ^{12}C

SERVIZIO RIPRODUZIONE DELLA
SEZIONE DI TRIESTE DELL'INFN

SINGLE NEUTRON EMISSION FOLLOWING THE π^- ABSORPTION AT REST IN ^{12}C

C. Cernigoi, N. Grion, G. Pauli and R. Rui

Istituto di Fisica, Università di Trieste, Italia

and

Istituto Nazionale di Fisica Nucleare, Sezione di Trieste, Italia

and

R. Cherubini

Istituto di Fisica, Università di Padova, Italia

and

Istituto Nazionale di Fisica Nucleare, Laboratori di Legnaro (Padova), Italia

and

D. Gill

TRIUMF, Vancouver B.C., Canada

Submitted for publication to Nuclear Physics

The non-radiative single neutron emission process following the π^--capture in nuclei plays an important role in the studies regarding the nuclear structure, the existence of π-condensation and Δ-isobars in atomic nuclei, as well as in the investigation of the pion absorption mechanism itself, particularly of the single nucleon absorption mechanism. Two other single nucleon emission processes are relevant to this regard, that is, the charge symmetric process (π^+,p) and the (π^-,p) process.

Theoretically, the single nucleon emission following the pion absorption is ascribed to either the absorption by an uncorrelated nucleon [1]) or to a mechanism of capture by a correlated pair of nucleons with the emission of one energetic nucleon while the other nucleon remains trapped in the nucleus [2]). Both these mechanisms have been studied and the different models predict rather different absorption rates.

Experimentally, the non-radiative single neutron emission following the absorption of negative pions at rest in nuclei heavier than ^{4}He (see ref. [3])) has been observed in rather few investigations. In fact, as far as we know, there are but two such investigations, i.e., that of Deutsch et al. [4]) regarding the ^{7}Li(π^-,n)^{6}He(g.s.) reaction and giving a yield of 1.8×10^{-2}, and that of Bassalleck et al. [5]) giving rates of $(1 - 2)\times10^{-3}$ per stopped pion for the (π^-,n) reaction on ^{6}Li, ^{7}Li and ^{12}C.

In this paper we present the results of a measurement of the inclusive energy spectrum of the neutrons, as well as of that of the protons, emitted after the absorption of negative pions at rest in ^{12}C. The high energy tail of the neutron spectrum exhibits a peak corresponding kinematically to the single neutron emission process $^{12}C(\pi^-,n)^{11}B$. The area under such peak gives an emission rate of $1.7x10^{-2}$ per stopped pion, which is about ten times greater than that reported in ref. [5]).

The neutron and the proton energy spectra have been measured during a kinematically complete experiment regarding the pion absorption at rest on ^{12}C that we have carried out at TRIUMF. The main purpose of the experiment was to study the emission of (n,n), (n,p), (n,d) and (n,t) pairs in time correlation with an event of capture at rest of a negative pion in the target [6]).

The single neutron emission is predicted to be a rather rare process with respect to other neutron-emitting channels of the pion absorption reaction. This fact implies some experimental difficulties concerning the background which, on the other hand, are partially compensated by the fact that the neutrons produced in the single neutron emission channel are expected to appear in the high energy region of the spectrum. In the specific case of ^{12}C the single neutron emission channel $\pi^- + {}^{12}C \rightarrow {}^{11}B + n$ gives a monokinetic neutron of 111.7 MeV (if the residual nucleus ^{11}B remains in its ground state), that is a value which is as much as 10 MeV greater than the kinematical limits of the two-particle emission channels (π^- ,nn) and (π^- ,np).

The experiment has been performed using the low energy $\pi-\mu$ channel M13 of the TRIUMF cyclotron [7]). This channel provides a pionic beam selectable in both momentum and intensity. For our experiment we have chosen a momentum of 113 MeV/c (corresponding to a pion energy of 40 MeV) with a momentum dispersion of 2.8% determined by the aperture of the horizontal slits of the beam transport system. Through the choice of such momentum a compromise between beam intensity and stopping rate of pions in the target was realized which was compatible with the use of a target thin enough to let the charged particles, produced in the absorption reaction, to escape from the target without a significant energy loss.

In fig. 1 our experimental set-up is shown. The target was a slab of graphite 0.204 gr/cm^2 thick. The rate of stopped pions was measured by means of a beam telescope very similar to that described in ref. [8]).

The neutrons were detected by means of four neutron counters and their energies were measured with the time-of-flight method. Each counter consisted of a NE 110 scintillator slab having an area of (200x15) cm^2 and a thickness of 5 cm. The performances of such counters are reported in ref. [9]). The four counters were arranged in two pairs and placed one on the top of the other in each pair. Each counter had its own electronics so that the four counters were working independently one from the other. So, it was possible to accumulate a higher statistics than by using only one counter, as well as to check the relative consistency of the behaviour of the counter pairs, which were located in zones of the experimental area characterized by different backgrounds. Because of their locations with respect to the beam telescope, and due to the presence of anticounters in the latter, the four neutron counters did not detect the charged particles.

The neutron time-of-flights were measured over a flight-path of 5.2 meters and with an overall time resolution of about 650 psec. This value of the time resolution was deduced from the energy resolution of 3.5 MeV associated with the peak of 90-MeV neutrons of the $\pi^- + {}^4He$ reaction measured in ref. [8]). Such overall time resolution was originated by (a) the intrinsic time resolution of the neutron counters measured with the beam electrons (see fig. 2), which included the time resolution of the beam telescope counter delivering the start signal (counter CT2 in fig. 1), and (b) the spread due to the different flight paths of the pions hitting the target as well as to the degrader effect (see ref. [10]). A rough estimation of the two contributions mentioned in (b) lead to a total value of the time resolution that was in agreement with the aforesaid value. Owing to the large dimensions of the neutron counters it was necessary to determine the momentum directions of the detected neutrons in order to take into account the differences in the lengths of the neutron flight-paths. This was performed by means of a time-of-flight technique, described in ref. [11]), which allowed the determination of the neutron momentum directions with an uncertainty of the order of 1 degree. The energy threshold of the neutron detectors was set at about 6 MeV for electrons, i.e., at about 11 MeV for protons. This was done by using the beam electrons and taking into account the equivalence in light output of electrons and protons in plastic scintillators according to the data of ref. [12]). Setting the threshold at higher values would not have improved the overall time resolution significantly. On the other hand, since the object of our experiment was to investigate the particle emission due to the direct reaction mechanisms of the pion absorption reaction, the chosen threshold was high enough to eliminate the low energy boiling-off neutrons emitted in the pion absorption processes as well as to suppress almost completely the low energy gamma rays coming from the deexcitation of the residual nuclei or from neutron captures and pion anelastic reactions. Finally, it has to be pointed out that a low energy cut at 14 MeV was introduced in the neutron energy spectrum by the computing program used off-line for handling the data.

The energy dependence of the efficiency of the neutron counters, for the chosen threshold, (see ref. [8]) was calculated using a MonteCarlo Code [13]. The calculated curve has been normalized to the experimental value for the 90-MeV neutrons of the (n,t) channel of the reaction $\pi^- + {}^4He$, as reported in ref. [8].

The protons were detected by means of a counter which is described in detail in ref. [11]. It is called range telescope in fig. 1. Such counter allowed the identification of the detected particles emitted following the pion absorption reaction, which were either neutrons or protons or heavier ions. The proton energies were measured with the time-of-flight method with a flight-path of 4.02 meters, and being the counter overall time resolution of the same order as that of the neutron counters. The energy threshold for the proton detection was set at 19 MeV as described in ref. [11].

In fig. 3 the measured inclusive neutron time-of-flight spectrum is shown. It results from the addition of the spectra of the four counters corrected for background (different for each counter) but not corrected with regard to the position of the detection point. The latter correction is not large and affects the spectrum structures negligibly. It has been introduced, anyway, in the energy spectrum, as pointed out below.

The part of the spectrum corresponding to the fastest neutrons is reported in fig. 4. To show the mutual consistency of the behaviour of the neutron counters, two of the components of the spectrum of fig. 4,as measured by one counter of each counter pair,are reported in fig. 5. Such spectra are not corrected at all, that is, they represent the straight output of the time-to-digital converter.

The spectrum of fig. 4 (or fig. 3) clearly exhibits a "prompt peak". This peak originates from gamma rays that are produced by charge exchange or radiative capture reactions induced by pions in the target itself as well as in the absorbing materials present around the target. Few electrons bypassing the electronic discrimination performed with the beam telescope as described in ref. [10]), may also contribute to such peak. So, the source of the particles responsible of this peak, although correlated in time with the pion absorption event, is not geometrically well defined but is distributed in the target region. This is why the fwhm of the peak is relatively large (1600 psec).

Apart from the prompt peak, in the spectrum of fig. 4 two other peaks are clearly present at 39 nsec and 42.5 nsec, respectively. Their positions on the time scale with respect to the prompt peak correspond to the time-of-flight values - calculated on the basis of the pure kinematics - pertaining to the 111.7-MeV neutrons emitted in the $\pi^- + {}^{12}C \rightarrow {}^{11}B + n$ reaction (38.7 nsec), and, respectively, to the 90-MeV neutrons emitted in the $\pi^- + {}^{4}He \rightarrow t + n$ reaction (42.5 nsec). The latter reaction is supposed to occur on an alpha-cluster of the structure of the ${}^{12}C$ nucleus.

The energy spectrum, corrected by taking into account the neutron impact point position, is shown in fig. 6. It exhibits structures at 111 MeV and 89 MeV corresponding to the two peaks in the time-of-flight spectrum at 39 nsec and 42.5 nsec, respectively.

The peak at 111 MeV, which is well above the kinematical end point of the (π^-,2n) reaction at 101 MeV, corresponds — as said above — to the single neutron emission reaction $^{12}C(\pi^-,n)^{11}B$, leading to the ^{11}B nucleus in its ground state or one of its low energy excited states. In fact, our energy resolution in this energy region is of about 4.5 MeV (fwhm value) and is not sufficient to separate the ground state of ^{11}B from its low energy excited states, if populated. It should be pointed out, also, that the neutrons contributing to this peak can be originated by the pion absorptions in the carbon nuclei of the target as well as of the scintillating medium of the beam-telescope counter which is located just before the target. Such counter (CM3 in fig. 1) is a plastic scintillator NE102A of (10x 10) cm^2 and 0.05 cm thick, located 16 cm before the target. The contribution due to this counter relative to that due to the target can be estimated from the ratio of the counter-to-target thicknesses. Such contribution is equal to $\sim$ 16%. (In this estimation it has been neglected the pion captures occurring in the air present between the counter and the target, which anyway do not involve carbon nuclei). The aforesaid contribution has been found also experimentally and is shown in fig. 7 by the dashed curve. In such figure the dashed curve appears shifted towards the higher energies with respect to the solid curve which represents the contribution due to the target. This shift is in agreement with the fact that the latter contribution is due to neutrons originated by pions stopped in the target, that is, 16 cm after the counter, or, about 1.5 nsec later than those stopped in the counter. The latter number is the estimated average time required by the pions to cover the counter-to-target distance. Furthermore, the difference in the neutron flight-paths from the counter or from the target to the neutron detectors is taken to be negligible.

The area under the peak at 39 nsec of fig. 4, that is, the area under the peak at 111 MeV of fig. 6, is equal to $(1.70 \pm 0.34) \times 10^{-2}$ neutrons per stopped pion, that is about ten times greater that the value reported in ref. [5]). Such discrepancy might be due to a different estimation of the energy dependence of the neutron detection efficiency at such high values of the neutron energies. Also the degree of accuracy with which the absolute number of stopped pions is determined may sensitively affect the evaluation of the peak area.

The less pronounced peak at 89 MeV can be attributed — as said before — to the $^{4}He(\pi^{-},n)t$ channel of the pion absorption reaction on an alpha structure of the ^{12}C nucleus. The fwhm of this peak ($\sim$ 10 MeV) is about three times larger than our energy resolution in this region, which is about 3 MeV. It is also larger than the fwhm ($\sim$3.5 MeV) of the peak due to the same reaction channel and exhibited by the neutron spectrum measured in ref. [8]), which concernes the pion absorption in a liquid helium target. This can be explained by considering that the alpha-cluster substructure that possibly exists in the ^{12}C nucleus is not to be necessarily identified with the structure of an ^{4}He nucleus. Furthermore, also the eventual inelastic interactions that the emitted neutron might have with the remaining nucleons of the ^{12}C nucleus, before emerging from the nucleus itself, should be taken into account.

In fig. 8 the single proton energy spectrum is shown. Remarkable differences in shape between this spectrum and the neutron spectrum of fig. 6 are evident. In fact, in the low energy region the neutron spectrum exhibits a much more complex structure than the proton spectrum. Furthermore, at the high energies the proton spectrum drops down more quickly than the neutron spectrum, terminating pratically at about 80 MeV and presenting no significant structures. This can be expected by taking into account that the probability per stopped pion for the single proton emission process $^{12}C(\pi^-,p)^{11}Be$ is equal to $(4.5 \pm 0.8) \times 10^{-4}$, as found by Coupat et al. [14]), that is, smaller by a factor of the order of one hundred with respect to the probability for the single neutron emission $^{12}C(\pi^-,n)^{11}B$ as found in the present work.

This result is very important for testing different models for the pion absorption process. In fact, such result could find an explanation, for example, in terms of quite different absorption mechanisms, that is, the one nucleon absorption mechanism $\pi^- + p \rightarrow n$ in the case of the single neutron emission [1]), and a more complicated mechanism in the case of the single proton emission in which a charge exchange absorption reaction is implied [15]). Another hypothesis consists in describing the single nucleon emission through the interaction of the pion with a nucleon pair [2]). In such case different possibilities should be considered. In fact, the nucleon which is emitted with all the available energy can be either the absorbing nucleon (single neutron emission), or the one correlated with the absorbing nucleon (either single proton emission or single neutron emission).

The various chances involve differently the (p,p) and (p,n) pairs. As a consequence the ratio of the single neutron emission to the single proton emission probabilities should reflect in some way the relative number of the (p,p) and the (p,n) correlated pairs existing in the capturing nucleus, and therefore it should be explained by the nuclear structure models.

A final result that can be drawn from the neutron spectrum of fig. 6 concernes the multiplicity of fast neutrons (above about 16 MeV). This turns out to be equal to 1.25 neutrons per stopped pion, in good agreement with the average value 1.4 reported in the literature [16]). Such number depends obviously on the low energy cut-off.

REFERENCES

1) R.M. Spector, Phys. Rev. 134B (1964) 101;

J. Le Tourneux, Nucl. Phys. 81 (1966) 665;

J. Le Tourneux and J.M. Eisenberg, Nucl. Phys. 87 (1966)331;

M.A. Troitskii, M.V. Koldaev and N.I. Chekunaev, JETP Lett. 25 (1977) 123;

H.J. Pirner, Phys. Lett. 69B (1977) 190.

2) Il-T. Cheon, Y. Sakamoto and C. Nguyen-Trung. Progr. Theor. Phys. 34 (1965) 574;

J. Hüfner, Phys. Lett. 21C (1975) 1;

H.C. Chiang and J. Hüfner, Nucl. Phys. A352 (1981) 442.

3) M.M. Block, T. Kikuchi, D. Koethe, J. Kopelman, C.R. Sun, R. Walker, C. Culligan, V.L. Telegdi and R. Winston, Phys. Rev. Lett. 11 (1963) 301.

4) J.P. Deutch, L. Grenacs, P. Igo-Kemenes, P. Lipnik and P.C. Macq, Phys. Lett. 26B (1968) 315.

5) B. Bassalleck, H.D. Engelhardt, W.D. Klotz, F. Takeutchi, H. Ullrich and M. Furic, Nucl. Phys. A319 (1979) 397.

6) C. Cernigoi, R. Cherubini, N. Grion, G. Pauli, R. Rui and D. Gill, Report INFN/AE-82/9.

7) C.J. Oram, J.B. Warren, F.M. Marshall and J. Doornbos, Nucl. Instr. 179 (1981) 95.

8) C. Cernigoi, I. Gabrielli, N. Grion, G. Pauli, B. Saitta, R.A. Ricci, P. Boccaccio and G. Viesti, Nucl. Phys. A352 (1981) 343.

9) C. Cernigoi, N. Grion, G. Pauli and B. Saitta, Nucl. Instr. 144 (1977) 479.

10) C. Cernigoi, N. Grion, G. Pauli and B. Saitta, Nucl. Instr. 165 (1979) 401.

11) C. Cernigoi, N. Grion, G. Pauli, R. Rui and R. Cherubini, accepted for pubblication by Nucl. Instr.

12) H.C. Evans and E.H. Bellamy, Proc. Phys. Soc. 74 (1959) 483; T.J. Gooding and D.G. Pugh, Nucl. Instr. 7 (1960) 189; R.L. Craun and D.L. Smith, Nucl. Instr. 80 (1970) 239

13) N.R. Stanton, Report COO-1545-92 (1971), Ohio State University.

14) B. Coupat, P.Y. Bertin, D.B. Isabelle, P. Vernin, A. Gerard, J. Miller, J. Morgenstern, J. Picard and B. Saghai, Phys. Lett. 55B (1975) 236.

15) J.M. Eisemberg and D.S. Koltun "Theory of Meson interaction with nuclei", J. Wiley, New York, 1980.

16) H.K. Walter, Proc. 7th Int. Conf. on High Energy Physics and Nuclear Structure, Zürich (Birkhäser, Basel, 1977).

FIGURE CAPTIONS

Fig. 1 Experimental set-up.

Fig. 2 Intrinsic time resolution of the neutron counters. The conversion factor is 40 psec per channel.

Fig. 3 Single-neutron time-of-flight spectrum.

Fig. 4 Time-of-flight spectrum of the fastest neutrons.

Fig. 5 Single-neutron time-of-flight spectra measured by the neutron counters NC2 and NC3.

Fig. 6 Single-neutron energy spectrum.

Fig. 7 Contributions to the neutron energy spectrum due to the beam-telescope counter CM3 (dashed curve) and to the carbon target (solid curve).

Fig. 8 Single-proton energy spectrum.

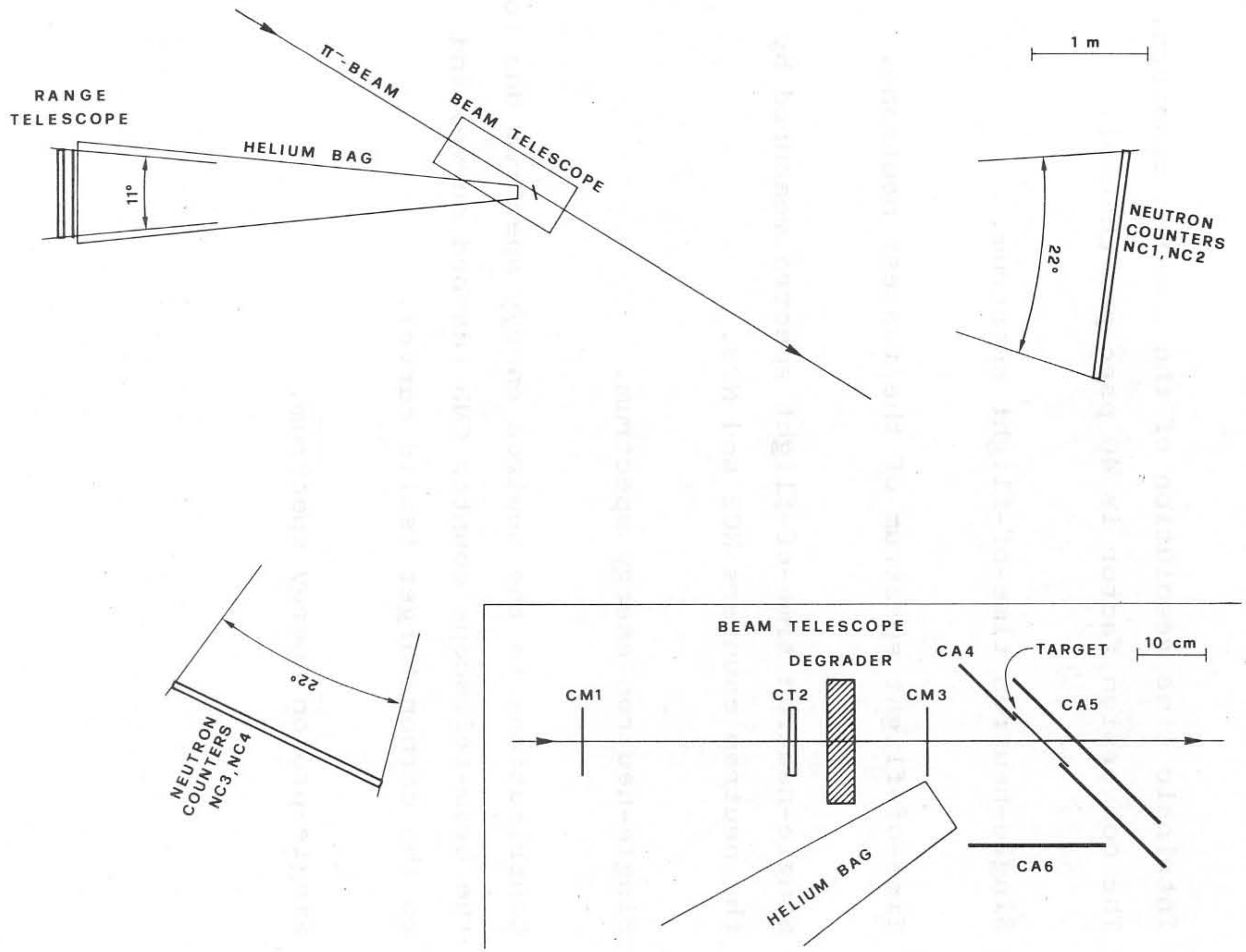
RANGE TELESCOPE
HELIUM BAG
11°
π^--BEAM
BEAM TELESCOPE
1 m
NEUTRON COUNTERS NC1, NC2
22°
NEUTRON COUNTERS NC3, NC4
22°
BEAM TELESCOPE
DEGRADER
CA4
TARGET
10 cm
CM1
CT2
CM3
CA5
CA6
HELIUM BAG

Fig. 1

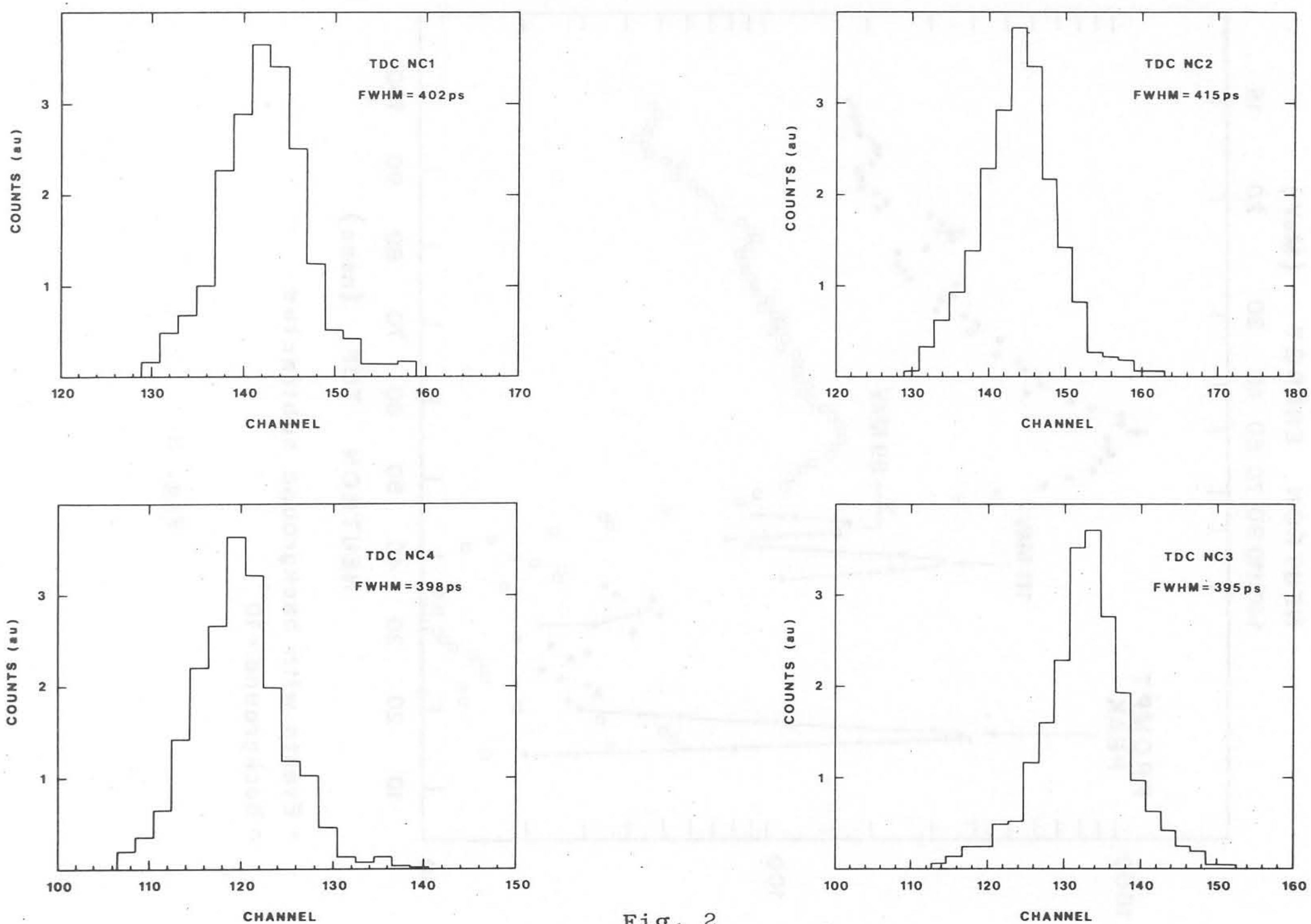
TDC NC1
FWHM = 402 ps
COUNTS (au)
CHANNEL
TDC NC2
FWHM = 415 ps
COUNTS (au)
CHANNEL
TDC NC4
FWHM = 398 ps
COUNTS (au)
CHANNEL
TDC NC3
FWHM = 395 ps
COUNTS (au)
CHANNEL

Fig. 2

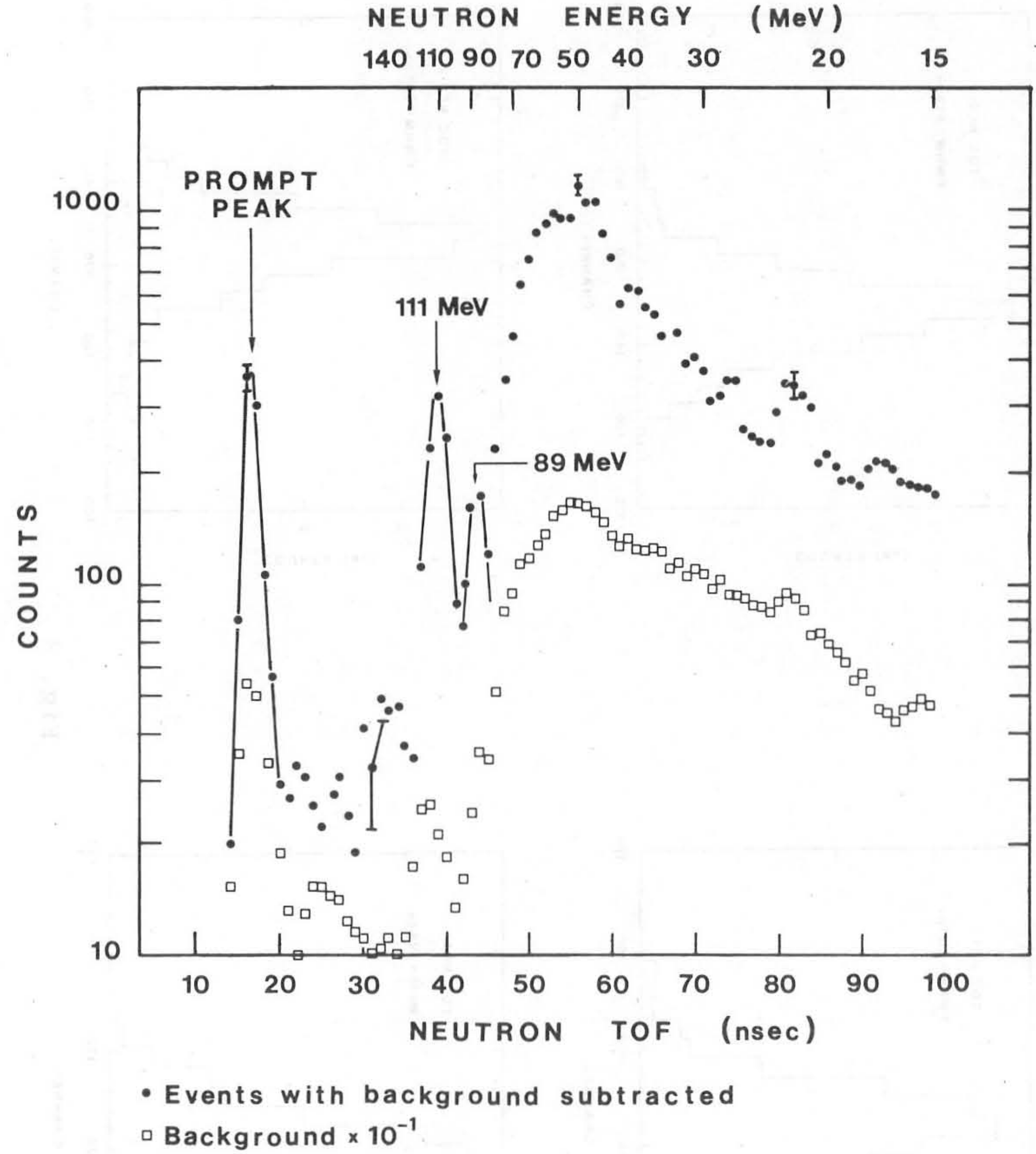

NEUTRON ENERGY (MeV)
140 110 90 70 50 40 30 20 15
PROMPT PEAK
111 MeV
89 MeV
COUNTS
1000
100
10
10 20 30 40 50 60 70 80 90 100
NEUTRON TOF (nsec)
• Events with background subtracted
□ Background × 10^{-1}

Fig. 3

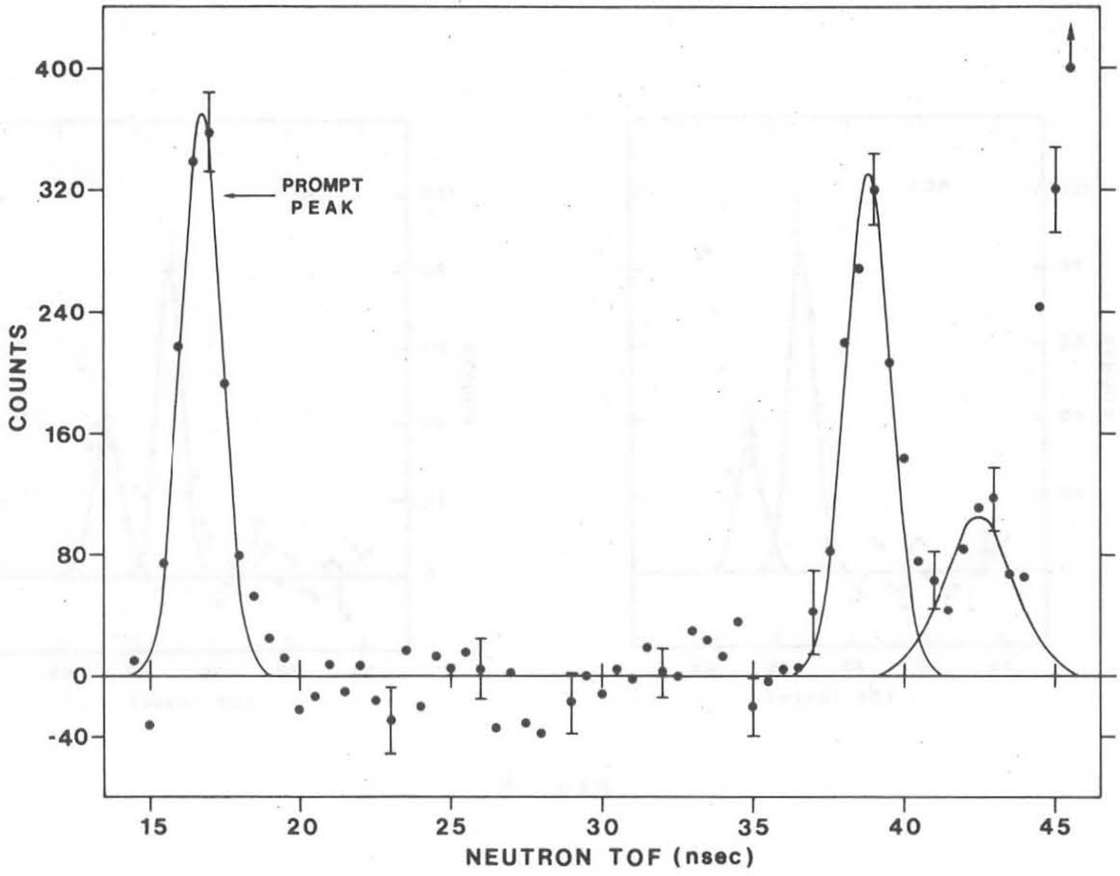
PROMPT
PEAK
COUNTS
400
320
240
160
80
0
-40
15
20
25
30
35
40
45
NEUTRON TOF (nsec)

Fig. 4

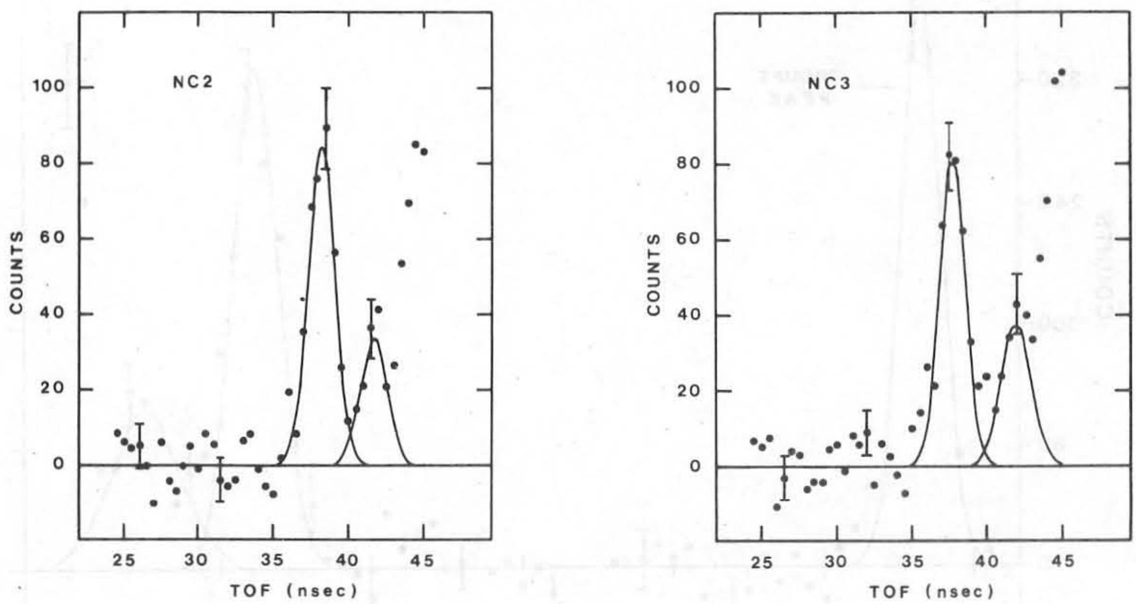
NC2
COUNTS
100
80
60
40
20
0
25
30
35
40
45
TOF (nsec)
NC3
COUNTS
100
80
60
40
20
0
25
30
35
40
45
TOF (nsec)

Fig. 5

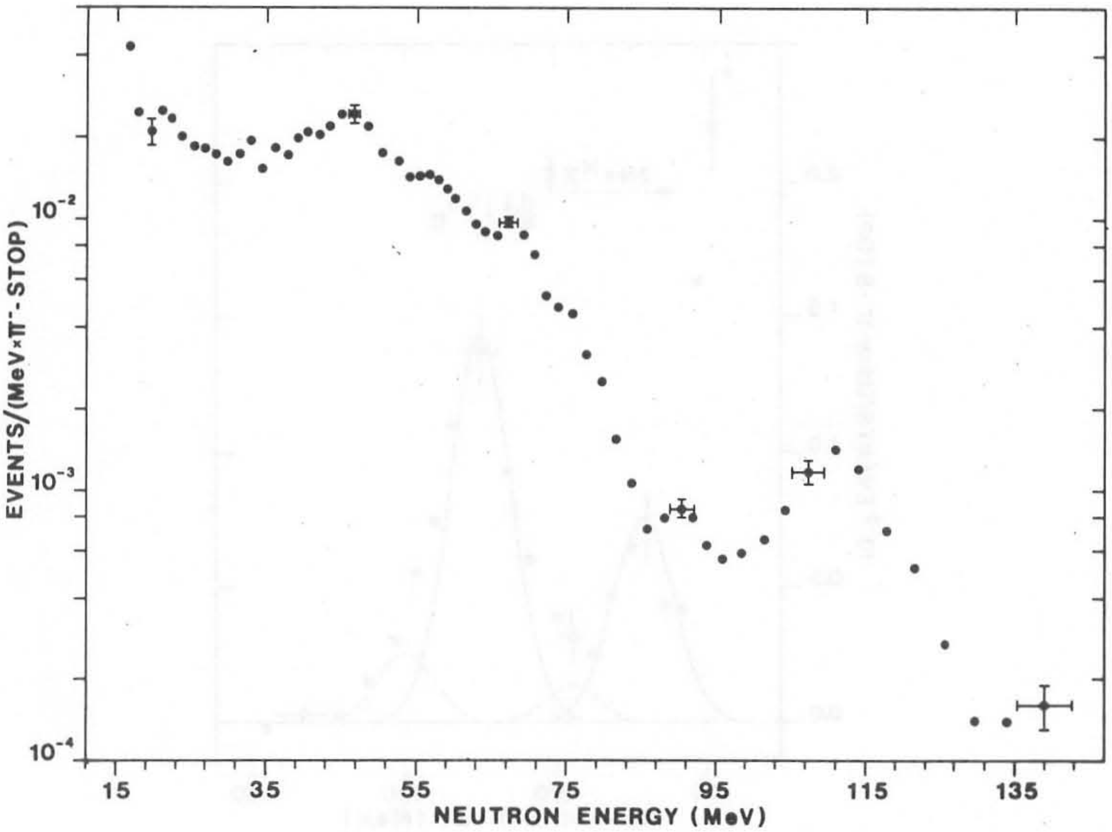
EVENTS/(MeV×π⁻-STOP)
10⁻²
10⁻³
10⁻⁴
15
35
55
75
95
115
135
NEUTRON ENERGY (MeV)

Fig. 6

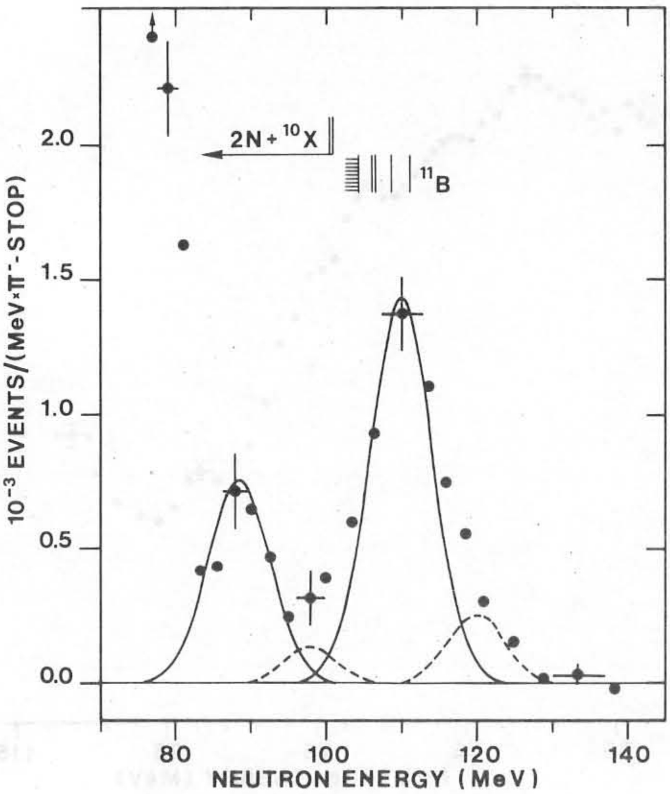

2N + ¹⁰X
¹¹B
10⁻³ EVENTS/(MeV×π⁻-STOP)
2.0
1.5
1.0
0.5
0.0
80
100
120
140
NEUTRON ENERGY (MeV)

Fig. 7

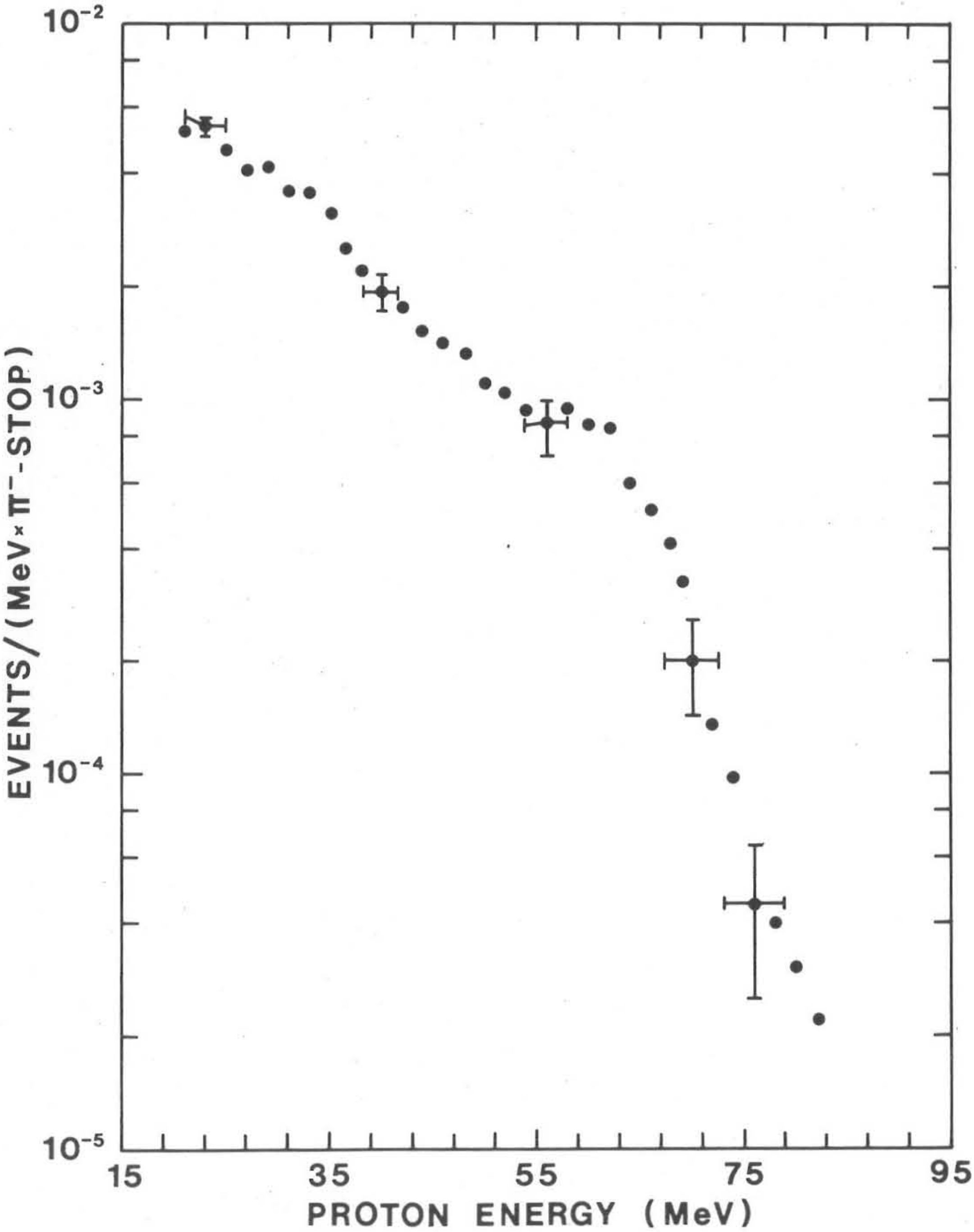

10^{-2}
10^{-3}
10^{-4}
10^{-5}
EVENTS/(MeV×π⁻-STOP)
15
35
55
75
95
PROTON ENERGY (MeV)

Fig. 8